Journal of Alloys and Compounds 731 (2018) 397–402

Contents lists available at ScienceDirect

Journal of Alloys and Compounds

journal homepage: http://www.elsevier.com/locate/jalcom

Magnetic structure of $La_{1-x}Tb_xMn_2Si_2$ compounds

E.G. Gerasimov [a, b, *], N.V. Mushnikov [a, b], P.B. Terentev [a, b], A.N. Pirogov [a, b]

[a] Institute of Metal Physics of UB RAS, S. Kovalevskaya str., 18, 620990 Ekaterinburg, Russia
[b] Institute of Natural Sciences and Mathematics, Ural Federal University, Mira str. 19, Ekaterinburg, Russia

ARTICLE INFO

Article history:
Received 17 May 2017
Received in revised form
24 August 2017
Accepted 8 October 2017
Available online 10 October 2017

Keywords:
Rare-earth intermetallics
Magnetic phase transitions
Exchange interactions
Magnetic anisotropy
Magnetic phase diagram

ABSTRACT

The magnetic structure of $La_{1-x}Tb_xMn_2Si_2$ compounds with $0 \leq x \leq 1$ has been studied by powder neutron diffraction and magnetization measurements on single-crystal samples. We demonstrate that at 4.2 K, with increasing the Tb concentration, a canted ferromagnetic structure of $LaMn_2Si_2$ changes at $x > 0.2$ to a canted antiferromagnetic structure. The antiferromagnetic in-plane component of Mn moment decreases with increasing concentration x and vanishes at $x > 0.5$. $TbMn_2Si_2$ is characterized by a collinear in-plane Mn ordering and ferrimagnetic structure, in which the Mn sublattice possesses the ferromagnetic interlayer alignment along the easy c-axis. Neutron diffraction study does not reveal a long-range magnetic order of Tb moments for the compounds with $x \leq 0.4$. Our results show that for concentrations $0.2 < x \leq 0.4$, a competition of the interlayer Tb-Mn, Mn-Mn exchange interactions and strong uniaxial magnetic anisotropy leads to formation of a frustrated magnetic state of Tb ions, which prevents magnetic ordering in the Tb sublattice.

1. Introduction

Intermetallic compounds RM_2X_2 (R is the rare earth element or Y; M is the 3d-, 4d-, or 5d-transition metal; X is Si or Ge) crystallize in the naturally layered body-centered tetragonal $ThCr_2Si_2$-type structure (space group $I4/mmm$). In this structure, mono-atomic layers of different elements are stacked along the crystallographic c-axis in the strict sequence -M-X-R-X-M-. The layered structure is considered to be responsible for quite an exciting variety of physical properties observed in these compounds [1,2].

Diversity of types of magnetic ordering and phase transitions were found in the RM_2X_2 compounds for M = Mn [1–3], where Mn atoms carry magnetic moment. Systematic study of different ternary and pseudoternary RMn_2X_2 compounds shows that the exchange interactions strongly depend on the in-plane Mn-Mn distance $d_{Mn\text{-}Mn}$. For the compounds with $d_{Mn\text{-}Mn} < d_c \approx 0.285$–$0.287$ nm, the axial component of Mn magnetic moments of adjacent Mn layers is ordered antiferromagnetically, while for $d_{Mn\text{-}Mn} > d_c$, the ferromagnetic ordering of the Mn magnetic moments of the Mn layers along the c-axis is realized [1,2,4]. Additionally, for several RMn_2X_2 systems with smaller lattice parameter a, the second critical distance $d_{c2} \approx 0.282$–0.284 nm was experimentally verified [5–7]. In the compounds with $d_{c2} < d_{Mn\text{-}Mn} < d_c$, both intralayer and interlayer magnetic couplings are antiferromagnetic, which leads to the formation of a canted antiferromagnetic structure. For the compounds with $d_{Mn\text{-}Mn} < d_{c2}$, no intralayer in-plane spin component is observed, Mn moments form a collinear ferromagnetic order within Mn monolayers, while the interlayer Mn-Mn coupling remains antiferromagnetic. Both the spontaneous and field-induced changes of the interlayer Mn-Mn magnetic ordering in the compositions with $d_{Mn\text{-}Mn} \approx d_c$ are accompanied by considerable volume and anisotropic lattice deformations [8]; therefore, the RMn_2X_2 compounds can be considered as materials for magnetostriction applications [9]. A variety of magnetic phase transitions makes these systems also attractive for magnetocaloric studies [10–14].

Acting upon the interatomic distances by means of external hydrostatic pressure [15,16] or “chemical pressure” in the quasi-ternary $R_{1-x}R'_xMn_2X_2$ and $RMn_2(Si_{1-x}Ge_x)_2$ systems [1–3,5–7] is considered to be a way to control magnetic structures and magnetic phase transitions in these compounds. Recently, we have performed magnetic measurements for the $La_{1-x}Tb_xMn_2Si_2$ system for which the lattice parameters decrease, while the Tb-Mn and Tb-Tb exchange interactions increase, with increasing x [17]. In this paper, in order to clarify the origin of different types of magnetic ordering in RMn_2X_2, we have studied magnetic structures of the $La_{1-x}Tb_xMn_2Si_2$ compounds for different x using powder neutron

* Corresponding author. Institute of Metal Physics of UB RAS, S. Kovalevskaya str., 18, 620990 Ekaterinburg, Russia.
E-mail address: gerasimov@imp.uran.ru (E.G. Gerasimov).

https://doi.org/10.1016/j.jallcom.2017.10.050
0925-8388/

diffraction and magnetization measurements on single-crystal samples.

2. Samples and experimental details

The alloys $La_{1-x}Tb_xMn_2Si_2$ with the concentration $0 \le x \le 1$ were prepared by induction melting of the constituents in an argon atmosphere followed by annealing at 900°C for one week. According to the powder X-ray diffraction analysis, all the studied alloys are single-phase with the tetragonal $ThCr_2Si_2$-type structure. For the magnetization studies, the quasi-single-crystal samples in the form of plates with the mass of 7–12 mg were selected from large grains of the ingot. X-ray back-scattered Laue analysis confirmed that the plates consist of several crystallites, the tetragonal *c*-axes of which are oriented strictly perpendicular to the plate plane, while the *a*-axes of crystallites are partially disoriented within the plane of the plate. In order to avoid rotation in magnetic field, the quasi-single crystals were glued in a cube of the epoxy resin, the *c*-axis of the samples being parallel to the cube edge.

The magnetization measurements of quasi-single-crystal samples were performed in the Center of Collective Use of IMP UB RAS with Quantum Design MPMS5-XL SQUID magnetometer in magnetic fields up to 50 kOe at different temperatures.

Neutron powder diffraction studies have been carried out at 4.2 and 293 K on the D-3 diffractometer with the neutron wavelength $\lambda = 0.2429$ nm at a horizontal channel of the IVV-2M reactor (Zarechny, Russia). The data were analyzed with the Rietveld-type refinement FullProf program.

3. Results and discussion

Based on the magnetic phase diagram of the $La_{1-x}Tb_xMn_2Si_2$ system obtained from magnetization measurements [17], we selected for neutron diffraction studies compositions with the Tb content $x = 0$, 0.1, 0.2, 0.27, 0.4, and 1.0. For these compounds, the ordering temperature for the Mn magnetic moments exceeds room temperature, while the Tb moments can order well below 100 K. Neutron diffraction patterns of all the selected samples collected at 4.2 and 293 K are given in Fig. 1. The diffraction patterns at 4.2 K contain the magnetic reflections originated from two magnetic sublattices, whereas at 293 K, only the Mn moments contribute to the magnetic neutron scattering.

Using the data of symmetry analysis [18] and the Rietveld refinement of neutron diffraction patterns, we determined magnetic structures which form in the $La_{1-x}Tb_xMn_2Si_2$ compounds at different Tb content. The structures are schematically shown in Fig. 2.

In $ThCr_2Si_2$-type structure (space group *I*4/*mmm*), nuclear and magnetic contributions to the observed intensities obey the following reflection conditions [3,5,6]:

(1) (*hkl*) with $h + k + l = 2n$ for nuclear reflections.
(2) (*hkl*) with $h + k + l = 2n$ and $h + k = 2n$ and $l = 2n$ for ferromagnetic ordering between the adjacent Mn planes (e.g. (112), (200) reflections).
(3) (*hkl*) with $h + k = 2n + 1$ for antiferromagnetic ordering of Mn atoms within the (001) planes (e.g. (101), (103) reflections).
(4) (*hkl*) with $h + k + l = 2n + 1$ for antiferromagnetic ordering between the adjacent Mn planes (e.g. (111), (113) reflections).

At 4.2 K (Figs. 1a and 2a) for $LaMn_2Si_2$, the reflections conditions (2) and (3) are satisfied, which corresponds to a canted ferromagnetic structure within the Mn layers and ferromagnetic interlayer

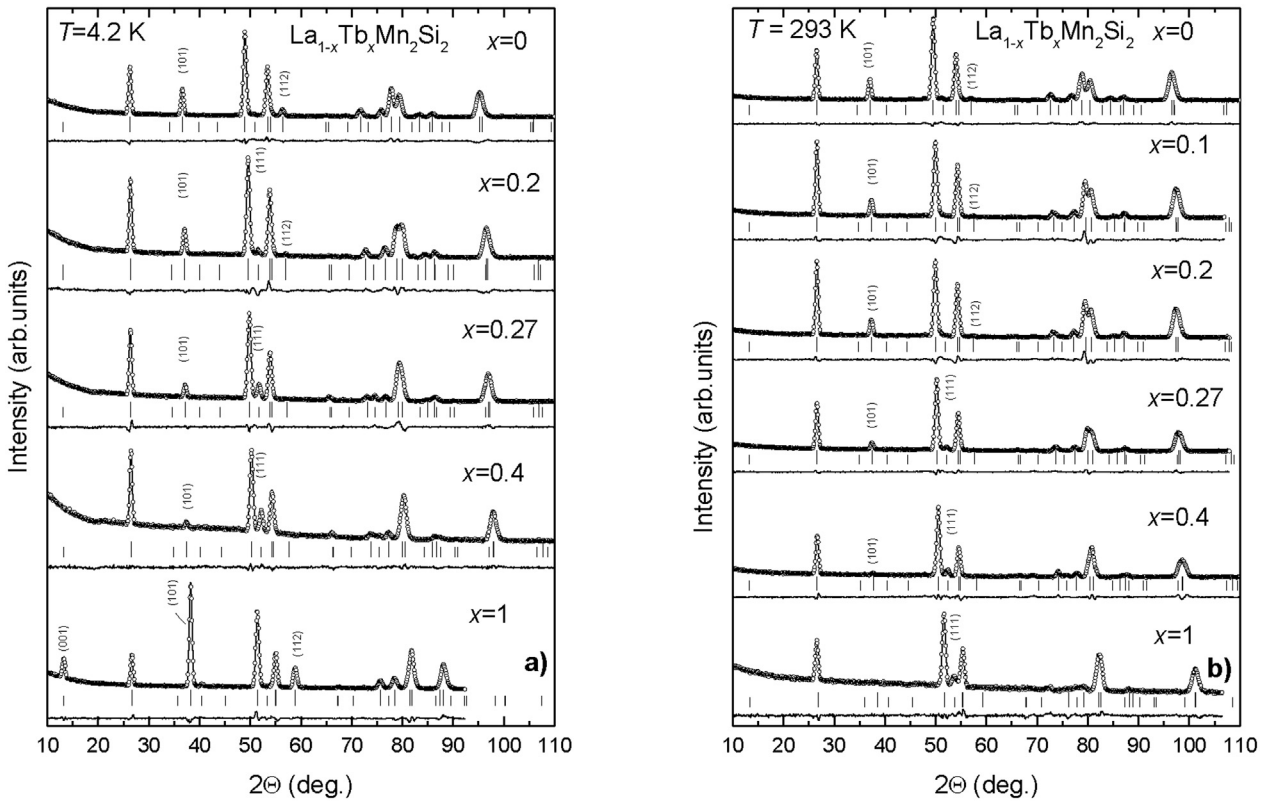

Fig. 1. Neutron diffraction patterns of $La_{1-x}Tb_xMn_2Si_2$ at 4.2 K (a) and 293 K (b). Points are experimental data, bold lines are Rietveld refinement with FullProf. Below the patterns, vertical lines point to the positions of magnetic and nuclear reflections, thin solid line shows the difference between the experimental and calculated patterns.

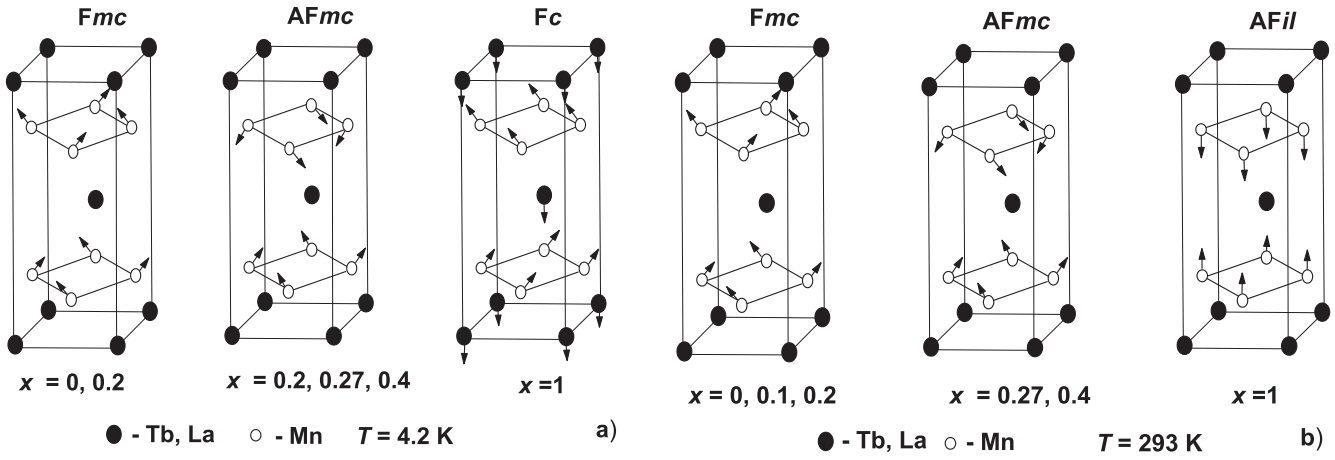

Fig. 2. Magnetic structures of $La_{1-x}Tb_xMn_2Si_2$ compounds at 4.2 K (a) and 293 K (b).

ordering (F*mc*) of axial components of the Mn moments directed along the *c*-axis, in agreement with the previously reported data [19]. For the $La_{1-x}Tb_xMn_2Si_2$ with $x = 0.27$ and 0.4, the interlayer ordering of the manganese moments is antiferromagnetic (the reflections conditions (3) and (4), the structure AF*mc*). The magnetic structure of the compound with $x = 0.2$ is interpreted as a mixture of phases with the ferromagnetic F*mc* and antiferromagnetic AF*mc* interlayer Mn-Mn couplings. For $TbMn_2Si_2$, the interlayer Mn-Mn ordering is found to be ferromagnetic again (in addition to the reflections condition (2) for the Mn sublattice, we observe an intensive reflection (101) from the Tb magnetic sublattice), with the negatively coupled Tb and Mn moments forming a ferrimagnetic (F*c*) structure [20,21]. Within the manganese layer, we observe canted magnetic structures with the antiferromagnetic ordering of the basal-plane components of Mn moments for all the studied compounds (the reflections condition (3)). The only exception is $TbMn_2Si_2$ for which the in-plane components of Mn moments of a monolayer order ferromagnetically.

At 293 K (Figs. 1b and 2b), in the compounds with $x = 0$, 0.1, and 0.2, the canted ferromagnetic interlayer ordering of Mn moments (F*mc*) is observed, which is confirmed by the reflections conditions (2) and (3). With further increasing of the concentration *x*, the interlayer ordering changes to the antiferromagnetic (AF*mc*) for $x = 0.27$ and 0.4. Within the manganese layer, we observe canted magnetic structures with the antiferromagnetic alignment of the basal-plane components of Mn moments for the compositions with $x = 0.27$ and 0.4 (the reflections conditions (3) and (4)), while in $TbMn_2Si_2$ all the Mn moments are oriented along the *c*-axis (the reflections condition (4), AF*il* structure).

Neutron diffraction patterns of the compounds with the ferromagnetic interplane coupling of the in-plane ferromagnetic components are characterized by the occurrence of magnetic contribution to the (112) reflection, while in the compounds with the antiferromagnetic interplane coupling of the in-plane ferromagnetic components there appears a magnetic contribution to the (111) reflection. As is seen from Fig. 1b, at $T = 293$ K neutron diffraction patterns of the compounds with $x \leq 0.2$ do not contain the (111) line, whereas the (112) line is reliably detected. Therefore, for these compositions, the ferromagnetic interplane coupling of Mn moments is formed. For $x \geq 0.27$, the line (111) appears, while the (112) line disappears. This feature corresponds to the antiferromagnetic interplane coupling of Mn moments. At elevated temperatures, when Tb magnetic moments are disordered, the magnetic contribution to the intensity of (101) line reflects only the value of the in-plane component of the Mn magnetic moments μ_x in the F*mc* and AF*mc* states. With increasing the Tb content, the intensity of the (101) line decreases (Fig. 1b), which corresponds to a decrease in the canting angle for the Mn moments.

At $T = 4.2$ K, the ferromagnetic interplane coupling is proved by observation of the (112) line for the compounds with $x \leq 0.2$ and $x = 1$ (Fig. 1a). For an intermediate Tb content, we observe the (111) line that is the characteristic of antiferromagnetic interplane coupling. Therefore, the type of interlayer Mn coupling changes twice with increasing *x*: first at $x_c \approx 0.2$ and then at $0.4 < x_{c2} < 1$ (Fig. 2a). The neutron diffraction pattern of the compound with $x = 0.2$ at 4.2 K contains both the (111) and (112) reflections; they point to a coexistence of the phases with the antiferromagnetic and ferromagnetic interplane couplings of Mn magnetic moments. The similar mixing of the AF*mc* and F*mc* phases was observed earlier in the quasi-ternary compounds $La_{0.8}Y_{0.2}Mn_2Si_2$ [22] and $CeMn_2Ge_{2-x}Si_x$ for the concentration range $0.6 < x < 1.25$ [6,7,23]. The phase separation is observed in the compounds in which the in-plane Mn-Mn distance is close to its critical value d_c and the temperature variation leads to a spontaneous AF-F phase transition. In these compounds, the magnetic state appears to be very sensitive to the lattice parameters. Even small local variations of the lattice parameters caused by a non-statistical distribution of substituting atoms and magnetoelastic distortions can lead to formation of the mixed-phase state. The sensitivity of X-ray diffraction analysis is usually insufficiently high for the detection of phase separation. Recent detailed structural studies of $CeMn_2Ge_{2-x}Si_x$ using synchrotron radiation, allow revealing the coexistence of the regions with the *a* lattice parameters distinguished only by 0.37% [6].

The neutron diffraction pattern of $TbMn_2Si_2$ at 4.2 K (Fig. 1a) contains an intense (001) reflection in contrast to diffraction patterns of other compounds. The origin of this reflection is due to a ferromagnetic interplane coupling of the axial components of the ferromagnetically aligned Mn moments in the layers and antiferromagnetic interplane coupling of the planar components. The corresponding canted ferrimagnetic structure F*c* of $TbMn_2Si_2$ is shown in Fig. 2a.

The relative intensity of the (101) line is rather small and decreases with increasing *x* for the patterns recorded both at 4.2 and 293 K. The only exception is $TbMn_2Si_2$ at 4.2 K, where the (101) line is the most intense. At first sight, this feature looks strange, since the (101) line includes the main magnetic contribution from Tb atoms. It is natural to expect that this contribution should gradually increase with increasing concentration *x*. In order to explain this contradiction. We have to assume that the Tb sublattice is in the

Table 1
Parameters of magnetic structure of $La_{1-x}Tb_xMn_2Si_2$ as determined from the Rietveld refinements to neutron diffraction patterns obtained at 4.2 K.

x	Magnetic structure	μ^x_{Mn} (μ_B)	μ^z_{Mn} (μ_B)	θ (deg)	μ_{Mn} (μ_B)	μ_{Tb} (μ_B)	R_{Bragg}	R_{magn}	χ^2
0	F*mc*	2.06(2)	1.81(3)	49	2.74(3)	–	5.41	5.21	4.10
0.2	F*mc*+AF*mc*	1.09(1)	0.91(2)	50	1.42(2)	0.3(5)	6.58	16.0	7.20
0.27	AF*mc*	1.15(3)	1.84(3)	32	2.18(3)	1.0(8)	4.81	10.8	4.90
0.4	AF*mc*	0.66(5)	2.08(3)	18	2.18(3)	0.7(6)	5.56	16.1	2.46
1.0	F*c*	1.27(2)	0.85(5)	56	1.53(3)	8.9(1)	4.44	5.24	5.64

paramagnetic state down to 4.2 K in the compounds with $x = 0.2$, 0.27, and 0.4.

Numerical results of the Rietveld refinement of the neutron diffraction patterns are listed in Tables 1 and 2. At 4.2 K, the value of the total magnetic moment of manganese atom μ_{Mn} decreases with increasing x from 2.73 μ_B in $LaMn_2Si_2$ down to 1.53 μ_B in $TbMn_2Si_2$. The exception is $x = 0.2$ compound containing two magnetic phases. In our opinion, the value of μ_{Mn} for this mixed-phase compound is underestimated. The axial component of the Mn moment μ^z_{Mn} and the planar component μ^x_{Mn} change non-monotonously with increasing the Tb content, since the canting angle θ with respect to the *c*-axis also changes. For the compounds with ferromagnetic interlayer Mn coupling, the axial component μ^x_{Mn} amounts to 0.85–1.81 μ_B, in agreement with the bulk magnetization measurements of quasi-single crystals [17] and previously reported results of neutron diffraction studies for binary $LaMn_2Si_2$ [19]. For ternary $TbMn_2Si_2$, the reported values of μ_{Mn} vary from 1.8 μ_B [20] up to 2.4 μ_B [21]. In the present study, the data on the Mn magnetic moment (1.53 μ_B) in $TbMn_2Si_2$ are more consistent with the value determined in Ref. [20]. The value of the Tb magnetic moment in $TbMn_2Si_2$ is very close to 9 μ_B characteristic of the free Tb^{3+} ion. On contrary, for the compositions with $x \leq 0.4$, the calculated Tb moment is found to be equal zero within the error of calculation.

It should be noted that in our previous paper [17], based on the results of bulk magnetization measurements, we suggested the formation of antiferromagnetic ground state in the Tb sublattice. However, the neutron diffraction data clearly show that at 4.2 K no long-range antiferromagnetic order of the Tb moments is formed in the compounds with $x = 0.27$ and 0.4.

The variation in the magnetic structure in $La_{1-x}Tb_xMn_2Si_2$ with concentration x at room temperature is in good agreement with the current view on the behavior of Mn coupling in RMn_2X_2. The in-plane Mn-Mn distance $d_{Mn\text{-}Mn}$ monotonously decreases with increasing x and passes through the critical values $d_c = 0.287$ nm at $x = 0.24$ and $d_{c2} = 0.284$ nm at $x = 0.5$. For the compounds with $d_{Mn\text{-}Mn} > d_c$, we observe the ferromagnetic Mn-Mn interplane coupling (F*mc*); in the compounds with $d_{c2} < d_{Mn\text{-}Mn} < d_c$, the interplane coupling is antiferromagnetic AF*mc*; and finally, for $d_{Mn\text{-}Mn} < d_{c2}$, the antiferromagnetic interplane coupling and collinear ordering of the moments in Mn layers (AF*il*) is formed.

The band structure calculations for the compounds with non-magnetic R atoms, $LaMn_2Si_2$ ($d_{Mn\text{-}Mn} > d_c$) and YMn_2Si_2 ($d_{Mn\text{-}Mn} < d_{c2}$), showed that the main difference in their electronic structure is the higher hybridization degree of the Mn 3d states with Si 3p and La 5d-states across the valence band in the Y-containing compound [24]. This could affect both the direct and superexchange inter- and intraplanar Mn-Mn interactions. A possible increase in the hybridization strength in $La_{1-x}Tb_xMn_2Si_2$ with decreasing the lattice parameters is consistent with the observed decrease in the Mn magnetic moment from 2.74 μ_B in $LaMn_2Si_2$ down to 1.53 μ_B in $TbMn_2Si_2$ (see Table 1).

Fig. 3 shows the concentration dependence of the canting angle of the Mn moments with respect to the *c*-axis. For low Tb content, the canting angle is larger at 293 K than at 4.2 K. It should be noted that slightly above room temperature, the canted ferromagnetic structure of $LaMn_2Si_2$ changes to the planar antiferromagnetism (AF*il*). In the concentration range $0.2 < x < 0.5$, the canting angle decreases down to zero. These data suggest that the transition from AF*mc* to AF*il* structure is of the second-order type.

The regularities of rearrangement of magnetic structure when the in-plane Mn-Mn distance passes through the critical values d_c and d_{c2} are observed also at $T = 4.2$ K. The transitions shift to slightly lower Tb concentrations due to a thermal contraction of the lattice. Additionally, the magnetic phase transitions in the Mn sublattice at low temperatures are strongly affected by magnetic interactions with the Tb atoms. Since for $x > 0.2$, both the Mn-Mn and Tb-Mn interactions are antiferromagnetic and each layer of the Tb/La atoms is located at equal distances from the upper and lower Mn layers, the magnetic state depends on the relative strength of these interactions. For low Tb content, the energy of the Tb-Mn exchange interaction $I_{Tb\text{-}Mn}$ is smaller than the energy of the Mn-Mn interaction $I_{Mn\text{-}Mn}$. Therefore, the Mn interlayer coupling is antiferromagnetic. Since both the Mn sublattice and Tb ions possess a strong uniaxial anisotropy [17,25,26], the magnetic moments of Tb atoms should be directed along the *c*-axis. The Tb atoms appear to be in a frustrated state with respect to the Tb-Mn interplane interactions. The in-plane Tb-Tb indirect exchange is probably too small to order magnetic moments within the Tb layers at 4.2 K. Therefore, the neutron diffraction data do not reveal appreciable Tb moments for $0.2 \leq x \leq 0.4$. When the Tb concentration further increases, the $I_{Tb\text{-}Mn}$ also increases. As soon as the condition $I_{Tb\text{-}Mn} > I_{Mn\text{-}Mn}$ satisfies for $x > 0.5$, the Mn moments are forced to couple ferromagnetically under the influence of an indirect positive Mn-Tb-Mn exchange, in spite of the in-plane Mn-Mn distance $d_{Mn\text{-}Mn}$ being below its critical value.

The disordering of the Tb magnetic moments can be evidenced by bulk magnetization measurements. Fig. 4 shows the field dependences of magnetic moment μ of the compounds with $x = 0.27$ and 0.4 measured along the easy *c*-axis and in the basal plane. The magnetization curves show neither hysteresis nor spontaneous magnetization, which points to the paramagnetic or antiferromagnetic ground state. A considerable anisotropy of magnetic moments is seen for both compounds. At 4.2 K, in magnetic fields applied along the *c*-axis the antiferromagnetic Mn sublattice should give very small contribution to magnetic susceptibility. The magnetization for the paramagnetic Tb sublattice can be described by the relationship:

$$\mu(H,T) = x g_J J \cdot B_J\left(\frac{g_J J \mu_B H}{k_B T}\right) \quad (1)$$

for isotropic paramagnet. Here, x is the Tb concentration, $g_J = 3/2$ is the Landé factor, $J = 6$ is the total quantum number for Tb^{3+} ion, μ_B is the Bohr magneton, k_B is the Boltzmann constant, $B_J(z)$ is the Brillouin function. As seen from Fig. 4a and b, equation (1) gives a reasonable explanation of the observed magnetization curves for 4.2 K.

For higher temperature $T = 25$ K, the field dependence of magnetization calculated with eq. (1) (solid line in Fig. 4) goes

Table 2
Parameters of magnetic structure of $La_{1-x}Tb_xMn_2Si_2$ as determined from the Rietveld refinements to neutron diffraction patterns obtained at 293 K.

x	Magnetic structure	μ^x_{Mn} (μ_B)	μ^z_{Mn} (μ_B)	θ (deg)	μ_{Mn} (μ_B)	μ_{Tb} (μ_B)	R_{Bragg}	R_{magn}	χ^2
0	F*mc*	1.70(1)	0.90(4)	62	1.92(3)	–	3.13	5.58	3.75
0.1	F*mc*	1.41(2)	0.54(9)	69	1.51(4)	0	4.29	5.62	6.11
0.2	F*mc*	1.42(2)	0.60(8)	67	1.54(4)	0	4.18	6.88	5.81
0.27	AF*mc*	0.95(2)	1.02(2)	43	1.39(2)	0	1.5	8.81	2.51
0.4	AF*mc*	0.31(9)	1.47(3)	12	1.50(4)	0	4.01	11.0	3.52
1.0	AF*il*	0.00(0)	1.83(3)	0	1.83(3)	0	8.01	19.1	2.82

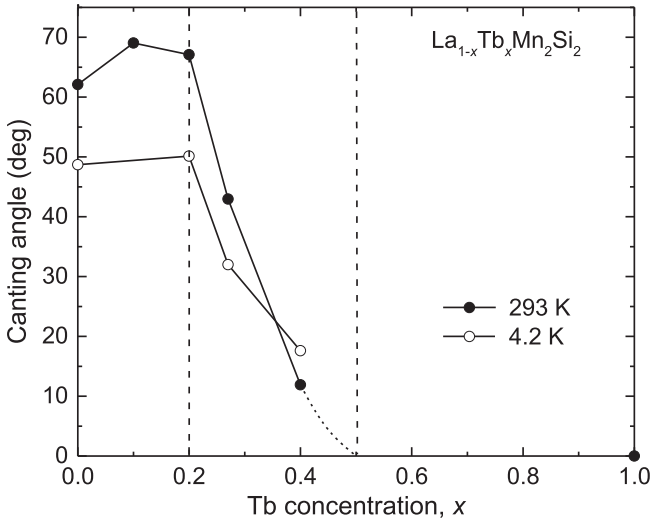

Fig. 3. Concentration dependences of the canting angle of the Mn moments with respect to the *c*-axis at 4.2 and 293 K.

much lower than that experimentally measured. This can be caused by the enhancement of the Tb-Mn interaction. The susceptibility of the antiferromagnetic Mn sublattice in the magnetic field directed along the *c*-axis is almost zero at 0 K and is expected to increase with increasing temperature. Even a small magnetic moment induced in the Mn sublattice will take off the frustrated state of the Tb moments and promote their ordering. To the best of our knowledge, there is no theory that explain the magnetization behavior for such a case. We can speculate that, besides the external field, in equation (1) there appears an additional field from the Tb-Mn interaction. In the linear approach, this additional field is proportional to both the external field and temperature. Then, eq. (1) can be rewritten in the form

$$\mu(H,T) = xg_J J \cdot B_J\left(\frac{g_J J \mu_B H(1+\nu T)}{k_B T}\right), \quad (2)$$

where ν is a numerical coefficient. Equation (2) describes well the magnetization curves at 25 K with the coefficient values $\nu = 0.05$ K^{-1} for $La_{0.73}Tb_{0.27}Mn_2Si_2$ and 0.04 K^{-1} for $La_{0.6}Tb_{0.4}Mn_2Si_2$ (dash-dot lines in Fig. 4a and b). For $T = 4.2$ K, both (1) and (2) give very similar magnetization values, because the νT product in (2) is small.

We recognize that equation (2) is applicable in a limited temperature range. Magnetic susceptibility of an anisotropic antiferromagnet along the antiferromagnetic axis is a nonlinear function of temperature, especially at low temperatures. As is shown above, the compounds studied have canted antiferromagnetic structure (AF*mc*), which should affect the *c*-axis susceptibility. The high-temperature limit also substantially differs from (2), since at high temperatures both magnetic sublattices contribute independently to the total susceptibility. Additional experimental and theoretical studies are needed to understand in details the magnetic behavior of the frustrated Tb sublattice in $La_{1-x}Tb_xMn_2Si_2$ compounds.

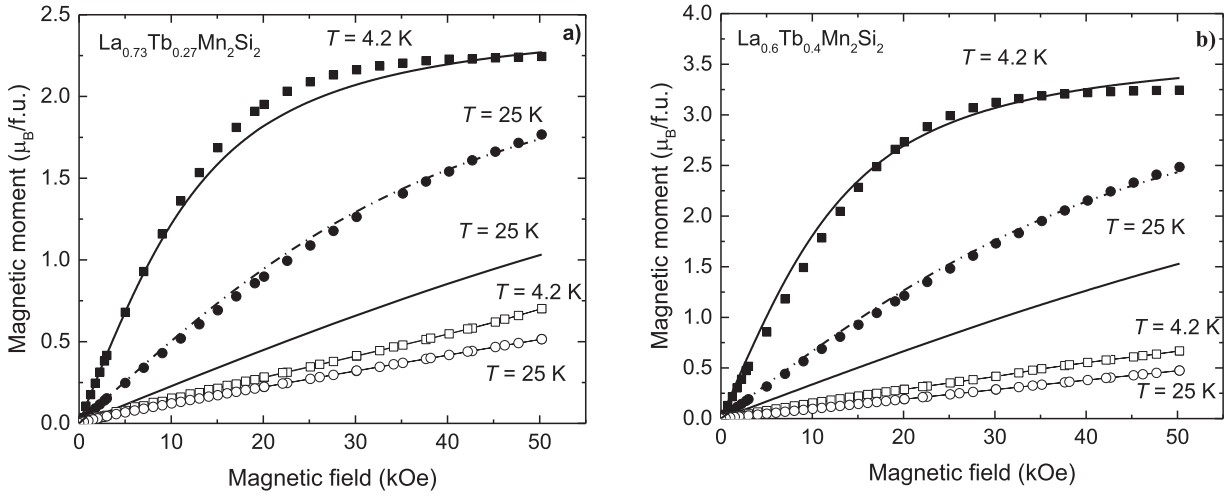

Fig. 4. Magnetization curves of $La_{0.73}Tb_{0.27}Mn_2Si_2$ (a) and $La_{0.6}Tb_{0.4}Mn_2Si_2$ (b) measured along the *c*-axis (closed symbols) and in the basal plane (open symbols) at temperatures 4.2 and 25 K. Solid lines are calculations with eq. (1) at 4.2 and 25 K. Dash-dotted line is magnetization calculated with eq. (2) at 25 K. For all calculations we used the values $J = 6$ and $g_J = 3/2$ for paramagnetic Tb^{3+} ions.

4. Conclusion

We have been performed powder neutron diffraction and magnetization measurements for quasi-single-crystals of the $La_{1-x}Tb_xMn_2Si_2$ compounds with $0 \leq x \leq 1$ to determine magnetic structures at 4.2 and 293 K.

At 293 K, for the $LaMn_2Si_2$, the in-plane Mn-Mn distance $d_{Mn\text{-}Mn}$ is higher than the critical value $d_c = 0.287$ nm, the interlayer Mn-Mn interaction is positive, and the magnetic structure is a canted ferromagnet. With increasing the Tb content and simultaneous decreasing the distance $d_{Mn\text{-}Mn}$, the interlayer Mn-Mn ordering changes twice: first time, from canted ferromagnetic to canted antiferromagnetic structure at $d_{Mn\text{-}Mn} = d_c$ ($x \approx 0.24$) and then, from canted to collinear antiferromagnetic structure at $d_{Mn\text{-}Mn} = d_{c2} = 0.284$ nm ($x \approx 0.5$). The behavior is in good agreement with the previously suggested model of existence of two critical in-plane Mn-Mn distances in RMn_2X_2 compounds.

At $T = 4.2$ K, magnetic interactions in the Mn sublattice also depend on the critical in-plane Mn-Mn distance. However, formation of magnetic structures in $La_{1-x}Tb_xMn_2Si_2$ is influenced by the interlayer Tb-Mn exchange interaction. The type of interlayer Mn-Mn order changes twice with increasing concentration x. In the compounds with $x \leq 0.2$, the average Mn magnetic moments of adjacent Mn layers are ordered ferromagnetically, whereas for $0.2 \leq x < 0.5$, antiferromagnetic Mn interlayer ordering is found. Finally, for higher Tb content, a reentrant ferromagnetic interlayer Mn-Mn ordering is formed due to the increase in the indirect positive Mn-Tb-Mn exchange interaction. In the intermediate concentration range $0.2 < x \leq 0.5$, no spontaneous magnetization was found in the bulk magnetization studies. We assume that for the compounds with $x = 0.27$ and 0.4, a competition of the interlayer Mn-Mn, Tb-Mn exchange interactions and strong uniaxial magnetic anisotropy of both the Tb and Mn sublattices leads to the formation of a frustrated magnetic state of the Tb moments, which prevents the long-range magnetic ordering in the Tb sublattice.

Acknowledgements

The study has been supported by Russian Science Foundation (project No. 15-12-10015). Neutron diffraction measurements have been performed at IMP Neutron Material Science Center within the state assignment of FASO of Russia (theme “Flux” No. 01201463334).

References

[1] A. Szytula, J. Leciejewicz, Handbook on the Physics and Chemistry of Rare Earths, vol. 12, 1989, p. 133.
[2] A. Szytuła, in: K.H.J. Buschow (Ed.), Handbook of Magnetic Materials, vol. 6, Elsevier, Amsterdam, 1991, p. 85.
[3] G. Venturini, R. Welter, E. Ressouche, B. Malaman, J. Magn. Magn. Mater. 150 (1995) 197–212.
[4] H. Fujii, T. Okamoto, T. Shigeoka, N. Iwata, Solid State Commun. 53 (8) (1985) 715–717.
[5] B. Emre, I. Dincer, M. Hoelzel, A. Senyshyn, Y. Elerman, J. Magn. Magn. Mater. 324 (2012) 622–630.
[6] M.F. Md Din, J.L. Wang, Z.X. Cheng, S.X. Doul, S.J. Kennedy, M. Avdeev, S.J. Campbell, Sci. Rep. 5 (2015), 11288-1-15.
[7] J.L. Wang, L. Caron, S.J. Campbell, S.J. Kennedy, M. Hofmann, Z.X. Cheng, M.F. Md Din, A.J. Studer, E. Bruck, S.X. Dou, Phys. Rev. Lett. 110 (2013) 217211.
[8] N.V. Mushnikov, E.G. Gerasimov, J. Alloys Compd. 676 (2016) 74–79.
[9] Y.Y. Gong, L. Zhang, Q.Q. Cao, D.H. Wang, Y.W. Du, J. Alloys Compd. 628 (2015) 146–150.
[10] E.G. Gerasimov, Yu. A. Dorofeev, V.S. Gaviko, A.N. Pirogov, A.E. Teplykh, Junghwan Park, J.G. Park, C.S. Choi, Unggirl Kong, Phys. Met. Metallogr. 94 (2) (2002) 161–169.
[11] N.V. Mushnikov, E.G. Gerasimov, P.B. Terentev, V.S. Gaviko, K.A. Yazovskikh, A.M. Aliev, Magn. Magn. Mater. 440 (2017) 89–92.
[12] Bibekananda Maji, Mayukh K. Ray, K.G. Suresh, S. Banerjee, J. Appl. Phys. 116 (2014) 213913.
[13] Chunsheng Fang, Guoxing Li, Jianli Wang, W.D. Hutchison, Q.Y. Ren, Zhenyan Deng, Guohong Ma, Shixue Dou, S.J. Campbell, Zhenxiang Cheng, Sci. Rep. 7 (2017), 45814-1-14.
[14] Guoxing Li, Jianli Wang, Zhenxiang Cheng, Qingyong Ren, Chunsheng Fang, Shixue Dou, Appl. Phys. Lett. 106 (2015) 182405.
[15] E.G. Gerasimov, N.V. Mushnikov, T. Goto, Phys. Rev. B 72 (2005) 064446.
[16] J. Kaštil, Z. Arnold, O. Isnard, Y. Skourski, J. Kamarád, J.P. Itié, J. Magn. Magn. Mater. 424 (2017) 416–420.
[17] E.G. Gerasimov, N.V. Mushnikov, P.B. Terentev, K.A. Yazovskikh, I.S. Titov, V.S. Gaviko, Rie Y. Umetsu, J. Magn. Magn. Mater. 422 (2017) 237–242.
[18] A.P. Vokhmyanin, A.N. Pirogov, Phys. Met. Metallogr. 115 (5) (2014) 457–464.
[19] M. Hofmann, S.J. Campbell, S.J. Kennedy, X.L. Zhao, J. Magn. Magn. Mater. 176 (1997) 279–287.
[20] T. Shigeoka, N. Iwata, H. Fujii, T. Okamoto, J. Magn. Magn. Mater. 54–57 (1986) 1343–1344.
[21] M. Kolenda, J. Leciejewicz, A. Szytula, N. Sttisser, Z. Tomkowicz, J. Alloys Compd. 241 (1996) L1–L3.
[22] M. Hofmann, S.J. Campbell, S.J. Kennedy, J. Phys. Condens. Matter 12 (2000) 3241–3254.
[23] J.L. Wang, S.J. Kennedy, S.J. Campbell, M. Hofmann, S.X. Dou, Phys. Rev. B 87 (2013) 104401.
[24] Dmitry M. Korotin, E.V. Rosenfeld, N.V. Mushnikov, E.G. Gerasimov, I.S. Zhidkov, A.I. Kukharenko, L.D. Finkelstein, S.O. Cholakh, E.Z. Kurmaev, J. Alloys Compd. 695 (2017) 1663–1671.
[25] E.G. Gerasimov, R.Y. Umetsu, N.V. Mushnikov, A. Fujita, T. Kanomata, J. Phys. Condens. Matter 19 (2007) 486202.
[26] E.G. Gerasimov, M.I. Kurkin, A.V. Korolyov, V.S. Gaviko, Phys. B 322 (2002) 297–305.